Northumbria Research Link

Performance Improvement of Brillouin Ring Laser based BOTDR System Employing a Wavelength Diversity Technique

Nageswara Lalam, *Student Member*, *IEEE*, Wai Pang Ng, *Senior Member*, *IEEE*, Xuewu Dai, *Member*, *IEEE*, Qiang Wu and Yong Qing Fu, *Member*, *IEEE*

Abstract—In this paper, a wavelength diversity technique is employed in a Brillouin optical time domain reflectometry (BOTDR) using a Brillouin ring laser (BRL) as a local oscillator. In the wavelength diversity technique, multiple wavelengths are injected into the sensing fiber, while the peak power of each wavelength is set below the nonlinear threshold level. This technique significantly maximizes the overall launch pump power, without activating the non-negligible nonlinear effects, which overcomes the limitation of the conventional BOTDR system. The BRL, which is simple and cost-effective, that can be used to reduce the receiver bandwidth in the order of few MHz. In addition, a passive depolarizer is used to reduce the polarization noise. The proposed system is validated experimentally over a 50 km sensing fiber with a 5 m spatial resolution. The experimental results demonstrate a signal-to-noise ratio improvement of 5.1 dB, which corresponds to 180% improvement compared to a conventional BOTDR system.

Index Terms— Wavelength diversity, distributed fibre sensors, Brillouin scattering.

I. INTRODUCTION

BRILLOUIN based distributed fiber sensors gained lot of attention in recent years, due to their immunity to electromagnetic interference, high sensing range over tens of kilometers, and capabilities of simultaneous strain and temperature measurements. The sensing mechanism is based on the linear dependence of Brillouin frequency shift (BFS) on strain and/or temperature along the fiber distance, while the sensing position is determined by the pulse time-of-flight method. In Brillouin-based distributed fiber sensors, two techniques are widely investigated: (a) Brillouin optical time-domain reflectometry (BOTDR) [1] based on spontaneous Brillouin scattering (SpBS); and (b) Brillouin optical time-domain analysis (BOTDA) [2] based on stimulated Brillouin scattering (SBS). The BOTDR features simple implementation schemes with accessing one end of the sensing fiber, while BOTDA allows higher sensing range, but requires access to the both ends of the sensing fiber [3].

Heterodyne detection is most commonly used in BOTDR/A system to improve the receiver sensitivity [4, 5]. The pump signal is injected into the one end of the sensing fiber, which generates SpBS signal and detected at the same end. The backscattered SpBS signal beats with the local oscillator (LO)

signal, and the resultant electrical beat signal has a frequency of about ~11 GHz (for silica based fibers), which requires the bandwidth of a photo-detector (PD) higher than 11 GHz. The use of higher bandwidth PD will result a higher noise equivalent power (NEP), which reduces the system accuracy. In addition, the higher bandwidth electronic devices are needed for electrical signal processing. To avoid the use of such high bandwidth devices, an intensity Mach-Zehnder modulator (MZM) is often employed in the LO path, while the modulated sideband frequency shift is controlled by the high bandwidth RF microwave generator. In this technique, the modulator needs to be precisely controlled and the system is complicated. Iida *et al*. [6] proposed a simple, cost-effective Brillouin ring laser (BRL) as a LO signal without using any expensive devices. Therefore, the receiver bandwidth can be reduced significantly in a cost-effective way.

The sensing performance is crucial in the BOTDR system. The signal-to-noise ratio (SNR) determines the performance of the BOTDR system. The increase of SNR significantly improves the sensing performance, which include the following reasons; (i) the sensing range: as the power decays exponentially over the fiber distance, the larger the SNR, the sensing range can be push further; (ii) spatial resolution: as the signal is proportional to the interaction length; (iii) measurement time: high SNR requires lower number of averages; (iv) higher measurement accuracy; and (v) higher frequency resolution [7]. The SNR is primarily governed by the injected pump power into the sensing fiber and the LO signal power. Increasing the injected pump power into the sensing fiber will improve the SNR but the level of the pump power is limited by the non-negligible nonlinear effects in the sensing fiber, which comprise of SBS and modulation instability (MI) [8]. If the pump power is above the nonlinear threshold, it will result in a depletion of the pump power and invoke unwanted nonlinear effects, hence reduce the sensing range and the accuracy of strain and temperature measurements [9]. On the other hand, if the LO signal power is strong enough, the SNR is no longer dependent on the LO signal power [10]. Several techniques have been proposed to improve the SNR of the BOTDR system, such as employing multiple longitudinal modes of Fabry-Perot laser [11], Raman amplification [12, 13] and pulse coding [14] techniques.

Considering the input pump power limitation and the complexity of the receiver bandwidth reduction, a novel wavelength diversity technique is employed together with a BRL in a conventional BOTDR system. The proposed system

can improve the SNR significantly with a simple implementation. In order to evaluate the sensing performance of the proposed system, the temperature effects have been measured using a 50 km sensing fiber with a 5 m spatial resolution.

II. COST-EFFECTIVE BANDWIDTH REDUCED BOTDR SYSTEM USING A BRILLOUIN RING LASER

In a heterodyne BOTDR system, the LO signal must have high coherency, low phase noise and sufficient peak power. The BRL output signal maintains a low phase noise and a high coherency with the Brillouin pump [15]. The schematic representation of the conventional BOTDR system using a BRL as a LO signal is illustrated in Fig. 1 [6]. The laser signal at a frequency of v_1 is divided into two propagation paths using a coupler, in which the upper path is used for the pulsed pump signal, whereas the lower path is used for the LO signal composed with a BRL. An erbium-doped fiber amplifier (EDFA) is used to pump the high peak power above the SBS threshold to obtain sufficient SBS power from the BRL fiber (10 km). In order to make sure the first order Stokes signal excited in the ring cavity, the isolator (ISO) is used [16]. The obtained SBS output signal has a frequency of v_1-v_{B-LO}. This Brillouin frequency is depends on the core material doping concentration [17]. The measured BRL Brillouin gain spectrum (BGS) has a peak frequency of 10.77 GHz with a narrow linewidth (full width at half maximum (FWHM)) of 5.2 MHz as shown in Fig. 2. The measured BRL optical spectrum is illustrated in Fig. 2 inset. The BRL peak power can be easily controlled using an EDFA. The detected beat Brillouin frequency is down-shifted in the order of few MHz, i.e,
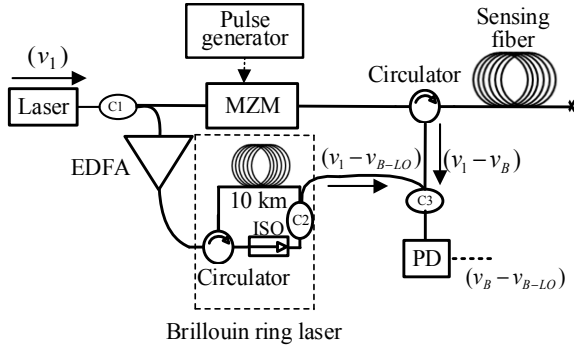

Fig. 1. Schematic representation of Brillouin ring laser based BOTDR (C=coupler, EDFA=erbium doped fiber amplifier, MZM= mach-zehnder modulator, ISO=isolator, PD=photodetector)
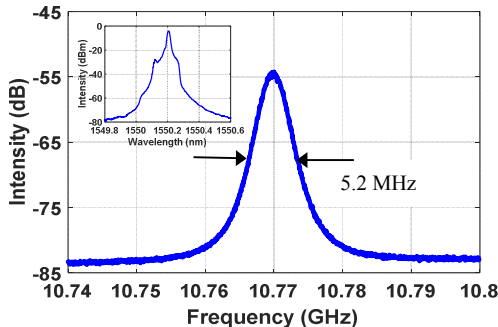

Fig. 2. Measured Brillouin gain spectrum of Brillouin ring laser (BRL). (inset: Measured optical spectrum of BRL output)

v_B-v_{B-LO}. For example, if the sensing fiber BFS is about v_B=10.88 GHz, and the BRL's BFS is v_{B-LO}=10.77 GHz, the resultant electrical beat frequency is v_B-v_{B-LO}=110 MHz. In this configuration, the BRL is composed with a simple implementation, and the bandwidth of PD and electronic devices can be reduced significantly.

III. OPERATING PRINCIPLE OF WAVELENGTH DIVERSITY TECHNIQUE IN BRILLOUIN RING LASER BASED BOTDR

In a wavelength diversity technique, multiple wavelengths are injected into the sensing fiber to improve the SNR, while peak power of each individual wavelength is kept below the nonlinear threshold level. As described in [18], the SBS threshold for N pump wavelengths is given by:

$$P_N^{th} = NP_1^{th} \qquad (1)$$

where, P_1^{th} is the single pump wavelength SBS threshold. Therefore, the SBS threshold with N wavelengths with equal power will be N times greater than the single wavelength. This technique enables the maximization of the total launch pump power into the sensing fiber and suppresses the nonlinear effects, the latter of which limits the BOTDR system performance. As a result, the SNR increases, thus improving the BOTDR system performance. The other nonlinear effects such as four-wave mixing and cross-phase modulation will not be excite in proposed system, as each wavelength pump power is less than the SBS threshold and pump pulse repetition frequency is normally less than 1 MHz [19, 20]. It is important to mention that, there are some prior works, such as employing a Fabry Perot laser [11] and multi-wavelength pump [19] using a polarization scrambler. Due to the large wavelength spacing (0.25 nm) between the Fabry Perot laser modes, the resultant beat spectrum significantly broadens, which leads to enormous BFS uncertainty. As proposed in [19], the MZM is employed in LO path for further shift the LO frequency of each wavelengths to reduce the receiver bandwidth. It is difficult to ensure the spectral quality and the stability of the modulated LO signals over time, moreover, a complicated and expensive design is required. In addition, the use of polarization scrambler induces the additional noise to the system. The proposed method by BRL and passive depolarizer significantly enhance the system performance with low cost and low complexity.

The concepts of the conventional BOTDR (single wavelength) and wavelength diversity BOTDR using a BRL are illustrated in Fig. 3 and Fig. 4, respectively. Fig. 3 illustrates the operating principle of the conventional BOTDR using a BRL with a frequency of v_1-v_{B-LO}. Fig. 4 illustrates our proposed wavelength diversity technique where three pump wavelengths (N=3) with the corresponding frequencies of v_1, v_2, v_3 have been considered for generating multiple pump wavelengths instead of a single wavelength in the conventional BOTDR. As shown in Fig. 4, the three pump wavelengths generate three BGS, which beat with the corresponding BRL signal and each pump wavelength has the same frequency separation (Δv) as shown in Fig. 4(b) [21]. Therefore, at the receiver, the Brillouin gain amplitude is superimposed (which is proportional to the sensor amplitude response [8]) as shown in Fig. 5. As a result, the SNR will increase.
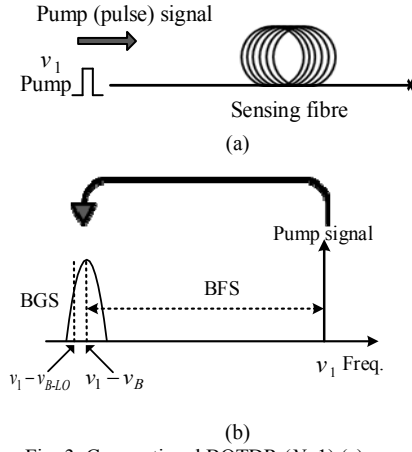
Fig. 3. Conventional BOTDR (*N*=1) (a) operating principle (b) Brillouin gain spectrum
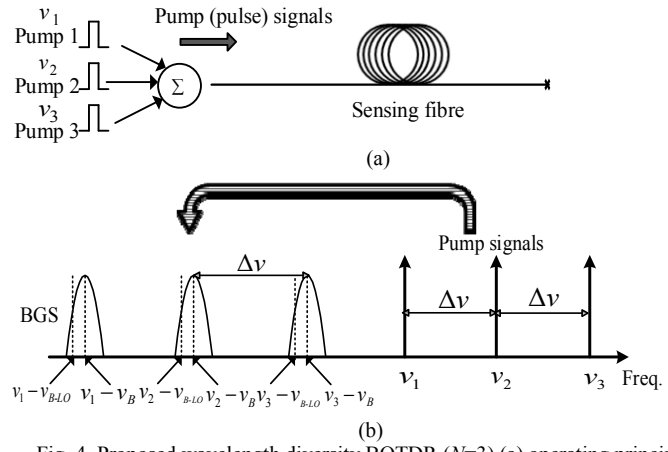

Fig. 4. Proposed wavelength diversity BOTDR (*N*=3) (a) operating principle (b) Brillouin gain spectrums
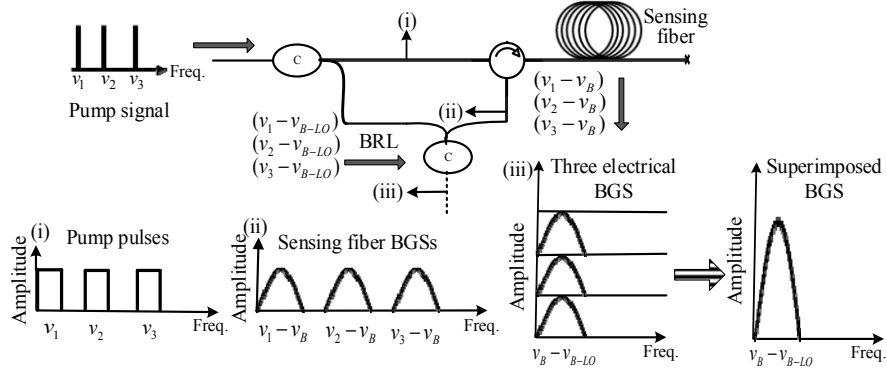

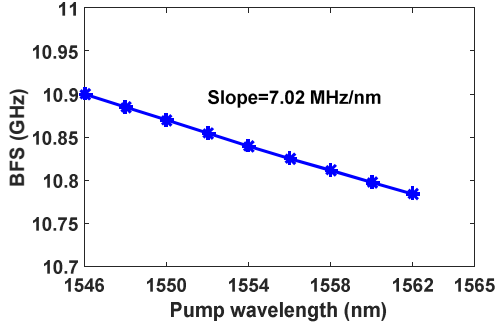Fig. 5. Schematic representation of proposed wavelength diversity BOTDR (*N*=3)

Fig. 6. Measured BFSs for wavelengths ranging from 1546 to 1562 nm

In this technique, the following factors should be taken into account: (i) the frequency spacing between the pump wavelengths should be greater than the PD bandwidth; (ii) the frequency spacing between the different pump wavelengths must be two times larger than the BGS linewidth of ~30 MHz to avoid the interference; (iii) on the other hand, if the frequency spacing is too large, it will result in a beat spectral broadening at the receiver, which causes a BFS uncertainty [22]. As shown in Fig. 6, we experimentally verified that the BFS dependence on pump wavelength. The measured BFS for different pump wavelengths ranging from 1546 to 1562 nm and the resultant BFS dependence is 7.02 MHz/nm. This corresponds to 0.056 MHz/GHz. In our proposed system, the beat spectral broadening at the receiver caused by the different pump wavelengths (Δ*v*=5 GHz) can be negligible negligible (which is 0.28 MHz compared to natural BGS linewidth of 30 MHz) due to the small frequency spacing of the pump wavelengths.

The detected photocurrent with N wavelengths can be expressed as [23]:

$$I_{\mathrm{ph}}(t) = 2R_D \sum_{i=1}^{N} \sqrt{P_{Bi}(t)P_{\mathrm{LO}i}} \cos(v_{Bi} - v_{\mathrm{LO}i})t \cos\theta(t) \qquad (2)$$

where, R_D is the photodetector responsivity, $P_{Bi}(t)$ is the peak Brillouin signal power of ith pump wavelength at time t, $P_{\mathrm{LO}i}$ is the peak power of ith LO signal, (v_{Bi}-v_{LO}) is the frequency difference between the Brillouin signal and LO signal, θ denotes the polarization angle difference of Brillouin signal and LO signal. Furthermore, the SNR of the wavelength diversity BOTDR with N wavelengths can be expressed as [19, 24]:

$$\mathrm{SNR}_N = \frac{2R_D^2 P_{T_B}(t)P_{T_{\mathrm{LO}}}}{(4k_{\mathrm{B}}TB/R_L) + (2qR_D P_{T_{\mathrm{LO}}}B) + <i_{\mathrm{E.noise}}^2>} \qquad (3)$$

where $P_{T_B}(t)$ is the total peak power of the Brillouin signal, $P_{T_{\mathrm{LO}}}$ is the total LO power and N_{avg} is the number of trace averages. In the above denominator, the first term $(4k_{\mathrm{B}}T/R_L)$ and the second term $(2qR_D P_{T_{\mathrm{LO}}}B)$ denote the thermal noise and shot noise of the photodetector, respectively. K_B is the Boltzmann constant, T is the photodetector operating temperature in Kelvin, R_L is the load resistance, q is the elementary charge, B is the bandwidth of the photodetector, the term $<i_{\mathrm{E.noise}}^2>$ is the power of the electrical noise from the signal acquisition system, such as electrical amplifier and electrical spectrum analyzer (ESA). In (3), the polarization state of both Brillouin signal and LO signal are assumed to be identical to each other (θ=0, a passive depolarizer is used in the proposed system).

$P_{T_B}(t)$ and $P_{T_{LO}}$ can be expressed as:

$$P_{T_B}(t) = \sum_{i=1}^{N} P_{Bi}(t) \qquad (4)$$

$$P_{T_{LO}} = \sum_{i=1}^{N} P_{LOi} \qquad (5)$$

where, $P_{Bi}(t)$ is the peak power of the Brillouin signal of ith pump wavelength and P_{LOi} is the peak power of the ith LO signal, respectively. In wavelength diversity technique, each pump wavelength has the same level of peak power, which is below the SBS/MI threshold. Therefore, the total injected pump power is spectrally distributed over three wavelengths to overcome the nonlinear effects.

IV. EXPERIMENTAL SETUP

The experimental setup for the wavelength diversity BOTDR using the BRL is shown in Fig. 7. A tunable distributed feedback (DFB) laser at a wavelength of 1550.116 nm with an output power of 10 dBm is used as a laser source. The single wavelength laser output is modulated by a MZM driven by an external microwave signal generator at 5 GHz. In order to stabilize the frequency spacing between the pump wavelengths, a specially designed bias controller circuit is used, which ensures a stable operation over time. By tuning the DC bias of the modulator, the three pump wavelengths (i.e., the carrier and two sidebands) can be set to an equal peak power. The three pump wavelengths are split into two propagation paths using 80/20 coupler 1, the upper branch signal is used for the pump and the lower branch signal is used for the LO signal. The polarization controller (PC) is employed at the input of each MZM to achieve the maximum optical power at the output of the MZMs. The upper branch signal is modulated with a dual drive MZM (DD-MZM), which modulates the electrical pulses into an optical pulse with a high extinction ratio (~42 dB). Subsequently, the output signal is amplified by an EDFA 1. An amplified spontaneous emission (ASE) filter is used to eliminate the ASE noise from the EDFA 1. A passive depolarizer [25] is employed to suppress the polarization noise in the proposed system. The polarization beam splitter (PBS) is used to split the input light polarization, which are orthogonal to each other. These two signals are coupled back though a polarization beam combiner (PBC). A polarization maintaining fiber (PMF) of 5 km is used as a delay fiber at one arm and a PC is inserted at another arm. The time delay between the two orthogonal polarization signals eliminates the fixed phase relationship between them, when they are recombined using the PBC. In this passive configuration, the pump signal is composed of two orthogonal polarization signals, which significantly eliminates the beat signal fluctuations [26, 27]. The LO signal is composed with a BRL as described in section 2. The EDFA 2 is used to obtain the sufficient peak power from the BRL. The BRL output consists of three Brillouin signals, which beat with the backscattered Brillouin signals of the sensing fiber. Finally, the received signal is detected by the balanced PD (bandwidth: 400 MHz) and amplified by a low noise RF amplifier (LNA), then analyzed by an electrical spectrum analyzer in a zero-span mode. Acquisition procedure and data processing remain identical to those of the conventional single wavelength BOTDR. The electrical signal from the PD consist summed contribution of BGS generated by three pump wavelengths.

V. RESULTS AND DISCUSSION

Firstly the BRL with three input wavelengths has been experimentally investigated. The three input wavelengths at a frequency of v_1, v_2, v_3 (Δv=5 GHz) and the three BRL output spectrums v_1-$v_{B\text{-}LO}$, v_2-$v_{B\text{-}LO}$, v_3-$v_{B\text{-}LO}$ are shown in Fig. 8. The BRL output consists of three SBS spectrums corresponds to three input pump wavelengths. The SBS peak powers can be easily adjustable using an EDFA 2. It is important to specify that, these optical spectrums are measured by an optical spectrum analyzer (OSA, AQ6370C) with a minimum resolution of 0.02 nm.

Thereafter, the sensing fiber SBS threshold was measured experimentally, which is ~18.2 dBm. For a reliable comparison, the peak power and pulse width of each pump wavelength are the same as those of the conventional single wavelength, i.e., 18 dBm and 50 ns, respectively. In order to experimentally validate the proposed system, the peak Brillouin frequency power traces are measured with a 50 km (two 25 km spools) fiber for both the conventional single wavelength BOTDR (N=1) and wavelength diversity BOTDR (N=3) using BRL. The SNR has been measured along the sensing fiber, then fitted with a polynomial curve in both the cases as shown in Fig. 9. At the
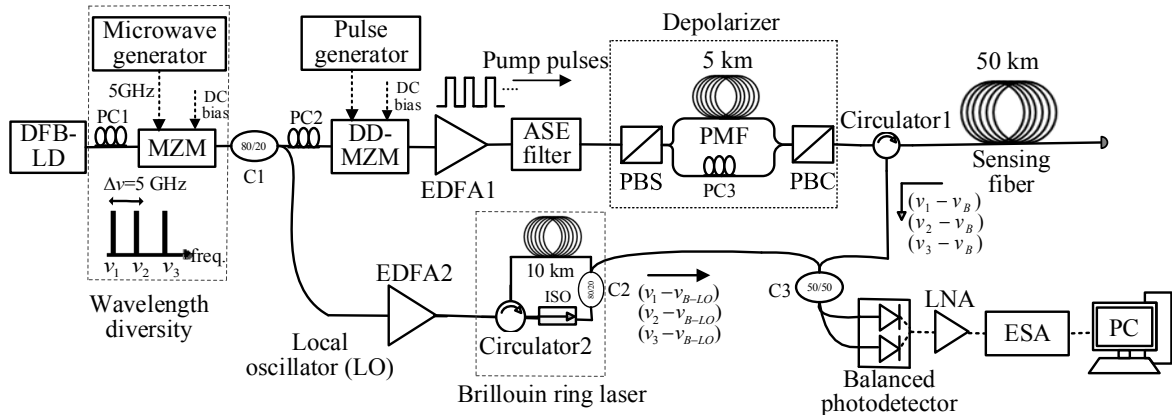

Fig. 7. Experimental setup of wavelength diversity BOTDR using Brillouin ring laser

(DFB= distributed-feedback laser, PC= polarization controller, MZM=mach-zehnder modulator, C=coupler, DD-MZM=dual drive-MZM, EDFA=erbium doped fiber amplifier, ASE=amplified spontaneous emission, PBS=polarization beam splitter, PBC=polarization beam combiner, PMF=polarization maintaining fiber, ISO=isolator, LNA: low noise RF amplifier, ESA=electrical spectrum analyzer)
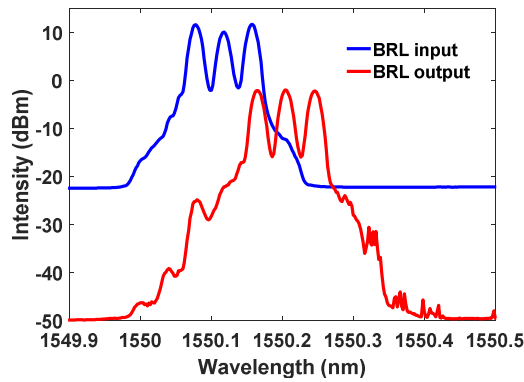
Fig. 8. The Brillouin ring laser input and output optical spectrums

end of the sensing fiber, the obtained SNR for the conventional BOTDR using the BRL is 3.6 dB. The proposed wavelength diversity BOTDR using the BRL is found to be 8.7 dB. Therefore, the improved SNR is 5.1 dB. For the wavelength diversity BOTDR (N=3), even with the high injected pump power, the measured SNR (blue trace in Fig. 9) has no distortions particularly from nonlinear effects and the pump power does not experience a power depletion, as the total power is spectrally distributed over the three wavelengths. Usually, in a BOTDR system, the balanced PD with a high trans-impedance amplifier is used to optimize the SNR of the obtained Brillouin gain traces. Therefore, it is worth to mention that the noise power level has been measured in both the cases,

for N=1 and N=3. The measured RMS voltage of the noise level is found to be same for the both cases, i.e., 71 µV with 2000 trace averages, as the system is dominated by the thermal noise [9]. Thus, the total noise level is same for the conventional BOTDR (N=1) and wavelength diversity BOTDR (N=3) using the BRL. The Brillouin gain spectrums at one fiber location are extracted in both cases and illustrated in Fig. 10. It can be clearly seen that the signal fluctuations are greatly reduced using the wavelength diversity technique.

The three-dimensional spectral mapping of proposed wavelength diversity BOTDR using the BRL is obtained with a scanning frequency step of 1 MHz and 2000 trace averages and illustrated in Fig. 11. The Lorenzian curve fitting is used for the obtained data and the measured BFS distribution over the fiber distance is shown in Fig. 11 inset. By calculating the standard deviation of the measured BFS at each fiber location, the BFS error along the fiber distance can be obtained. The standard deviations have been measured for the BFS along the sensing fiber for conventional BOTDR (N=1) and wavelength diversity BOTDR (N=3) using BRL, and the results are illustrated in Fig. 12. At the end of the sensing fiber, the BFS errors for the two cases are measured to be 1.75 and 0.52 MHz, respectively. Therefore, at the far end of the sensing fibre, the estimated accuracy of strain measurement is 35 µε and 10 µε, respectively (the calibrated strain coefficient of the sensing fiber is 0.05 MHz/µε). The temperature measurement accuracies are 1.6ºC and 0.5ºC, respectively (the calibrated temperature coefficient is 1.07 MHz/ºC).
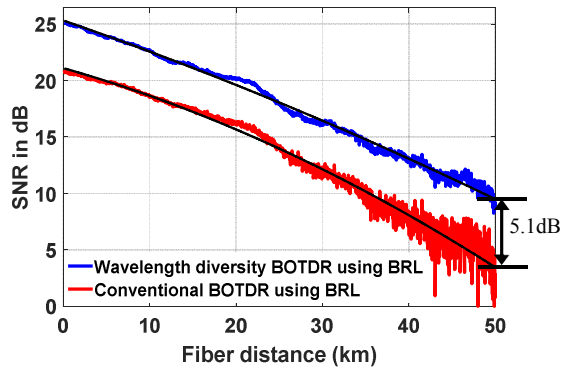

Fig. 9. Measured signal-to-noise ratio (SNR) at peak Brillouin gain frequency of conventional BOTDR (red curve), wavelength diversity BOTDR (blue curve) using Brillouin ring laser (BRL)

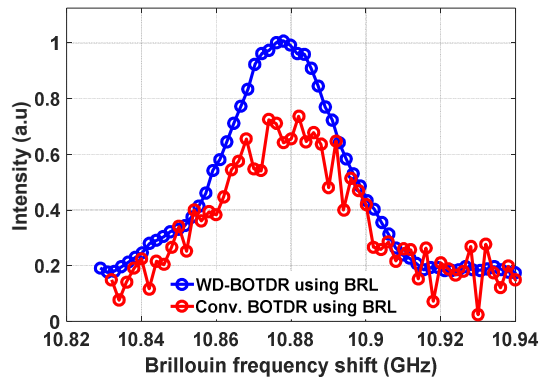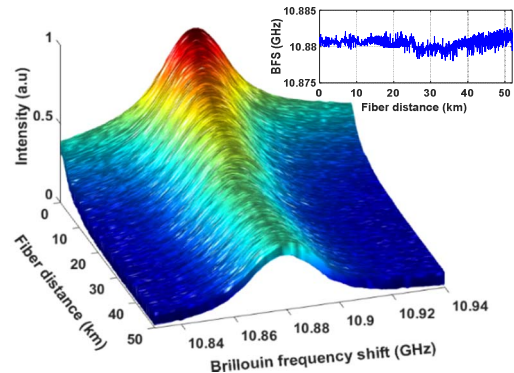Fig. 11. Brillouin gain spectrum over sensing fiber distance

Fig. 10. Measured Brillouin gain spectrums at end of the sensing fiber of conventional BOTDR and wavelength diversity BOTDR using Brillouin ring laser
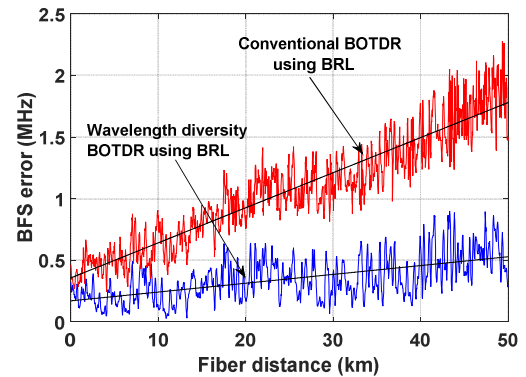

Fig. 12. Brillouin frequency shift (BFS) error vs fiber distance of conventional BOTDR and wavelength diversity BOTDR using Brillouin ring laser
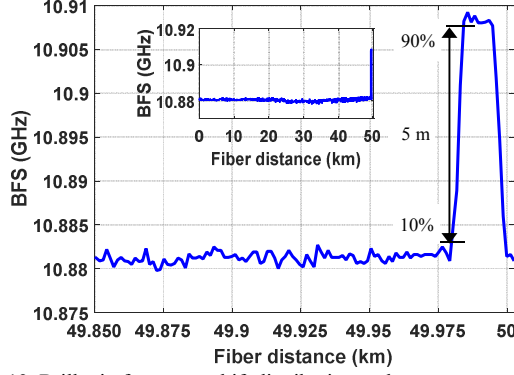
Fig. 13. Brillouin frequency shift distribution under temperature effects on 20 m fiber at end of the sensing fiber

The sensing performance and spatial resolution are characterized experimentally for the proposed wavelength diversity BOTDR using BRL. At the end of the sensing fiber, a 20 m fiber is kept in the temperature oven, while the rest of the fiber is kept at strain free and ambient room temperature (~25°C). The temperature was set at 50°C within the oven. The BFS distribution along the whole sensing fiber is shown in Fig. 13 inset. The spatial resolution of 5 m is obtained as shown in Fig. 13. The results demonstrate an accurate temperature measurement without any sacrifice on the spatial resolution in wavelength diversity technique.

TABLE I

PARAMETERS USED FOR THEORETICAL CALCULATION OF SNR IMPROVEMENT

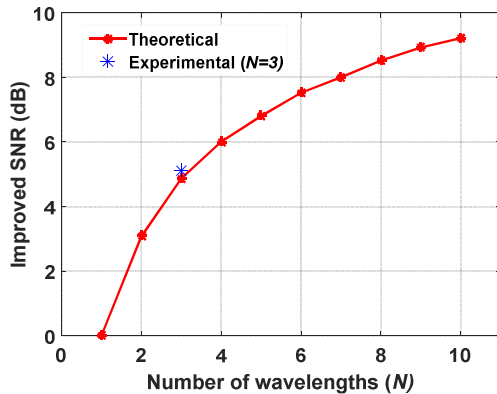| Parameter	Symbol	Value
Photodetector responsivity	R_D	1 (A/W)
No. of wavelengths	N	3
Local oscillator (LO) power	P_{LO}	2.5 dBm (1.77mW)
Boltzmann constant	k_B	1.38×10^{-23} (J/K)
Thermodynamic temperature	T	300 (K)
Photodetector bandwidth	B	400 MHz
Load resistance	R_L	50 (Ω)
Elementary charge	q	1.6×10^{-19} (c)
Electrical (signal acquisition) noise	$<i_{E.noise}^2>$	4×10^{-13} (A²)

Fig. 14. Improved SNR vs number of wavelengths

Considering the values listed in Table I and the data calculated using Eq. (3), (4) and (5), the theoretical SNR improvement compared to a single wavelength (N=1) BOTDR is illustrated in Fig. 1. For the proposed system (N=3), the obtained theoretical SNR improvement is 4.92 dB, which is in a good agreement with the experimental result of 5.1 dB. As shown in Fig. 14, the SNR improvement rate decreases as the number of wavelengths increases. This is because of the shot noise increases with increased Brillouin and LO signal power. The number of wavelengths can be increased by either multi EOMs or narrow spacing multi wavelength laser source, however the system will become more complex.

VI. CONCLUSION

We proposed and experimentally demonstrated a wavelength diversity technique employed in Brillouin ring laser based BOTDR system to improve the SNR. The wavelength diversity technique significantly maximizes the launch pump power, without activating the nonlinear effects, which limits the conventional BOTDR system performance. Whereas, the BRL significantly reduces the receiver bandwidth in the order of a few MHz. The frequency scan, acquisition procedure and data processing all remain identical to those of the conventional BOTDR system. In addition, considering the complexity and expensive methods required for polarization noise suppression in the BOTDR system, a simple, low-cost passive depolarizer is employed to reduce the polarization noise. Using the proposed technique, we can realize a SNR improvement of 5.1 dB compared to a conventional BOTDR with a spatial resolution of 5 m. The proposed system can be effectively combined with other sophisticated techniques, such as pulse coding and Raman amplification techniques for further improvement of sensor performance.

REFERENCES

[1] T. Kurashima, T. Horiguchi, H. Izumita, S. Furukawa, and Y. Koyamada, "Brillouin optical-fiber time domain reflectometry," *IEICE Trans. Commun,* vol. E76-B, 1993.
[2] T. Horiguchi, T. Kurashima, and M. Tateda, "Tensile strain dependence of Brillouin frequency shift in silica optical fibers," *IEEE Photonics Technology Letters,* vol. 1, pp. 107-108, 1989.
[3] R. Alan, "Distributed optical-fibre sensing," *Measurement Science and Technology,* vol. 10, p. R75, 1999.
[4] X. Bao and L. Chen, "Recent Progress in Distributed Fiber Optic Sensors," *Sensors,* vol. 12, pp. 8601-8639, 2012.
[5] D. Iida and F. Ito, "Detection Sensitivity of Brillouin Scattering Near Fresnel Reflection in BOTDR Measurement," *Journal of Lightwave Technology,* vol. 26, pp. 417-424, 2008.
[6] D. Iida and F. Ito, "Cost-effective bandwidth-reduced Brillouin optical time domain reflectometry using a reference Brillouin scattering beam," *Applied Optics,* vol. 48, pp. 4302-4309, 2009.
[7] M. A. Soto and L. Thévenaz, "Modeling and evaluating the performance of Brillouin distributed optical fiber sensors," *Optics Express,* vol. 21, pp. 31347-31366, 2013.
[8] M. Alem, M. A. Soto, and L. Thévenaz, "Modelling the depletion length induced by modulation instability in distributed optical fibre sensors," in *23rd International Conference on Optical Fiber Sensors*, Spain, 2014, pp. 91575S-91575S-4.
[9] M. A. Soto, A. L. Ricchiuti, L. Zhang, D. Barrera, S. Sales, and L. Thévenaz, "Time and frequency pump-probe multiplexing to enhance the signal response of Brillouin optical time-domain analyzers," *Optics Express,* vol. 22, pp. 28584-28595, 2014.
[10] X. Zhang, Y. Lu, F. Wang, H. Liang, and Y. Zhang, "Development of fully-distributed fiber sensors based on Brillouin scattering," *Photonic Sensors,* vol. 1, pp. 54-61, 2011.

[11] M. A. Soto, G. Bolognini, and F. D. Pasquale, "Distributed optical fibre sensors based on spontaneous Brillouin scattering employing multimode Fabry-Perot lasers," *Electronics Letters,* vol. 45, pp. 1071-1072, 2009.

[12] Y. T. Cho, M. Alahbabi, M. J. Gunning, and T. P. Newson, "50-km single-ended spontaneous-Brillouin-based distributed-temperature sensor exploiting pulsed Raman amplification," *Optics Letters,* vol. 28, pp. 1651-1653, 2003.

[13] M. N. Alahbabi, Y. T. Cho, and T. P. Newson, "Simultaneous temperature and strain measurement with combined spontaneous Raman and Brillouin scattering," *Optics Letters,* vol. 30, pp. 1276-1278, 2005.

[14] M. A. Soto, G. Bolognini, and F. D. Pasquale, "Analysis of optical pulse coding in spontaneous Brillouin-based distributed temperature sensors," *Optics Express,* vol. 16, pp. 19097-19111, 2008.

[15] R. Wang, L. Zhou, and X. Zhang, "Performance of Brillouin optical time domain reflectometer with erbium doped fiber amplifier," *Optik - International Journal for Light and Electron Optics,* vol. 125, pp. 4864-4867, 2014.

[16] D. Iida and F. Ito, "Low-Bandwidth Cost-Effective Brillouin Frequency Sensing Using Reference Brillouin-Scattered Beam," *IEEE Photonics Technology Letters,* vol. 20, pp. 1845-1847, 2008.

[17] M. Nikles, L. Thevenaz, and P. A. Robert, "Brillouin gain spectrum characterization in single-mode optical fibers," *IEEE Journal of Lightwave Technology,* vol. 15, pp. 1842-1851, 1997.

[18] Y. Aoki and K. Tajima, "Stimulated Brillouin scattering in a long single-mode fiber excited with a multimode pump laser," *Journal of the Optical Society of America B,* vol. 5, pp. 358-363, 1988.

[19] C. Li, Y. Lu, X. Zhang, and F. Wang, "SNR enhancement in Brillouin optical time domain reflectometer using multi-wavelength coherent detection," *Electronics Letters,* vol. 48, pp. 1139-1141, 2012.

[20] R. Hui and M. O'Sullivan, "Fiber Optic Measurement Techniques," ed: Academic Press, Elsevier, 2009, pp. 82-202.

[21] N. Lalam, W. P. Ng, X. Dai, Q. Wu, and Y. Q. Fu, "Performance improvement of BOTDR system using wavelength diversity technique," in *25th International Conference on Optical Fiber Sensors (OFS)*, Korea, 2017, pp. 1032366-1032366-4.

[22] H. Lee, N. Hayashi, Y. Mizuno, and K. Nakamura, "Observation of Brillouin gain spectrum in optical fibers in telecommunication band: Effect of pump wavelength," *IEICE Electronics Express,* vol. 13, pp. 1066-1076, 2016.

[23] Y. Li, X .Li, Q .An, and L. Zhang, "Detrimental Effect Elimination of Laser Frequency Instability in Brillouin Optical Time Domain Reflectometer by Using Self-Heterodyne Detection," *Sensors,* vol. 17, p. 634, 2017.

[24] A. Zornoza, M. Sagues, and A. Loayssa, "Self-Heterodyne Detection for SNR Improvement and Distributed Phase-Shift Measurements in BOTDA," *IEEE Journal of Lightwave Technology,* vol. 30, pp. 1066-1072, 2012.

[25] F. Wang, C. Li, X. Zhao, and X. Zhang, "Using a Mach–Zehnder-interference-based passive configuration to eliminate the polarization noise in Brillouin optical time domain reflectometry," *Applied Optics,* vol. 51, pp. 176-180, 2012.

[26] X. Zhang, R. Wang, and Y. Yao, "Brillouin optical time domain reflectometry using a reference Brillouin ring laser," in *22nd International Conference on Optical Fiber Sensors*, China, 2012, pp. 84219G-84219G-4.

[27] Y. Cao, Q. Ye, Z. Pan, H. Cai, R. Qu, Z. Fang*, et al.*, "Mitigation of polarization fading in BOTDR sensors by using optical pulses with orthogonal polarizations," in *23rd International Conference on Optical Fiber Sensors*, Spain, 2014, pp. 915764-915764-4.